

Diagnostic Value Of Doppler Ultrasound In Early Chronic Kidney Disease

Yanli Huang

The First Affiliated Hospital of Dalian Medical University

Xiaohang Wu

The First Affiliated Hospital of Dalian Medical University

Ye Tao

The First Affiliated Hospital of Dalian Medical University

Jialing Wu

The First Affiliated Hospital of Dalian Medical University

Yumei Yan

The First Affiliated Hospital of Dalian Medical University

Mengyan Ma

The First Affiliated Hospital of Dalian Medical University

Xinyue Yuan

The First Affiliated Hospital of Dalian Medical University

Fengfei Li

The First Affiliated Hospital of Dalian Medical University

Xui-kun Hou (✉ xkh912@sina.com)

The First Affiliated Hospital of Dalian Medical University

Research Article

Keywords: acoustic pulse radiative force imaging, chronic kidney disease, early diagnosis chronic kidney, pathological assessment, renal interlobar artery, ultrasonography examination

Posted Date: July 8th, 2021

DOI: <https://doi.org/10.21203/rs.3.rs-667000/v1>

License:  This work is licensed under a Creative Commons Attribution 4.0 International License.

[Read Full License](#)

Abstract

Objective: To explore of ultrasound combined with renal pathology score, and compare the application value of elastography, two-dimensional (2D) ultrasound, three-dimensional 3D ultrasound and other ultrasound imaging methods in early chronic kidney diagnosis.

Methods: Combined ultrasound and pathological scores. A retrospective analysis of 118 patients with chronic kidney disease examined in the department of nephrology of the author's hospital. 36 healthy who were normal in the same period were selected as the control group. Combined with the left kidney pathology score and multi-factor logistic regression analysis to evaluate independent predictors of early pathological injured in CKD, ROC curve analysis to evaluate the diagnostic efficacy of each ultrasound index. Statistical evaluation: The difference was statistically significant ($P < 0.05$).

Results: In patients with severely injured CKD, renal length, three-dimensional kidney volume, Renal interlobar artery RI, and AT all appear to be effective predictors. Among patients with moderate injured, only AT and RI were effective predictors. Among patients with mildly impaired CKD, AT has the highest diagnostic efficacy, but SWV has the highest sensitivity (83.8%) for detecting mild renal injured. The results confirm that the Renal interlobar artery AT is the strongest independent predictor of CKD injured.

Conclusion: The results confirm that the Renal interlobar artery AT is the strongest independent predictor of CKD injured.

Introduction

Chronic kidney disease (CKD) is a worldwide clinical and public health problem (¹Bello et al., 2017; ²Meola et al., 2008). It is a risk factor for cardiovascular and cerebrovascular diseases and gradually becomes a cause of morbidity and mortality (³Li et al., 2008; ⁴Muntner et al., 2012). This seriously increases the responsibilities of the existing health care system (⁵Mandayam., 2017). According to the Global Kidney Disease Health Survey of 2017, the different regions of the world show significant differences in the attention to and care of kidney diseases, which means that the detection and treatment levels of renal diseases in different regions are different. Therefore, the early detection of renal diseases and the implementation of secondary prevention are of vital importance to alleviate the progress of renal diseases and renal failure (⁶Boor et al., 2007; ⁷de Amorim et al., 2014).

At present, early detection and disease monitoring of CKD patients rely on imaging studies. In imaging studies, such as CT and PET / CT scans, the use of contrast agents increases the burden on the kidneys of patients, and even leads to an increase in patient morbidity and mortality. Due to the high cost of MRI, it cannot be used for routine examination of CKD. Traditional CKD diagnostic indicators, such as serum creatinine, urea nitrogen, and proteinuria, are not highly sensitive to the diagnosis of CKD and may lead to longer time intervals before successful intervention. Early treatment of CKD is very important to delay the progress of renal failure. There are no effective indicators for early detection of CKD. Therefore, it is

necessary to improve the early detection rate and timeliness of ultrasound examination as a routine examination method for kidney disease (⁸ Nightingale, 2011).

An imaging method that detects tissue elasticity, acoustic radiation force pulse imaging (ARFI) is another new, non-invasive method used to evaluate tissue hardness. In ARFI, the acoustic pulse exerts a set of pulses on the tissue over a short time, generating transverse shear wave propagation. The obtained tissue displacement is plotted based on the ultrasonography correlation method (⁹Nightingale et al., 2002). In theory, the propagation speed of shear waves is proportional to the density of tissues and the shear modulus in completely uniform and isotropic targets. ARFI has been most commonly used to detect liver-related diseases, but it is also used to detect pancreas-related diseases, among others (¹⁰Su et al., 2018; ¹¹Brancaforte et al., 2011). There is no study for the significance of ARFI, 3d ultrasonography 84 and other ultrasonography imaging methods in the detection of early chronic kidney disease. This is the first study to prove the relationship between the prolongation of renal interlobar artery AT and chronic renal injured. However, the significance of ARFI, three-dimensional (3D) ultrasonography and other ultrasonography imaging methods in the detection of early CKD remains to be further studied.

The purpose of this study was to compare the evaluation of early CKD by multiple ultrasonography imaging methods, such as elastography, two-dimensional (2D) ultrasonography and three-dimensional ultrasonography, by combining the renal pathology score.

Materials And Methods

Shortlisted Criteria

This study is a retrospective observational study. From April 2017 to May 2018, a total of 118 patients (male: female = 67:51, age 18–79) were examined in the Department of Nephrology of the First Affiliated Hospital of Dalian Medical University, and 36 normal volunteers with healthy physical examination during the same period As a control group.

These patients were recruited according to the following inclusion criteria: (1) Patients met the guidelines formulated by the National Kidney Foundation of the United States in 2002 under the Kidney Disease Prognosis Quality Initiative (K/DPQI). Under this initiative, CKD was defined as kidney injured for any reason or estimated glomerular filtration rate (e-GFR) below 60 ml/min/1.73 m for more than 3 months. (2) Patients agreed to receive ARFI, 3D imaging and renal biopsy. (3) Patients had one of the following indications: proteinuria, hematuria, nephrotic syndrome or injured renal function. Tips: Patients with hyperlipidemia, uric acid, or hypertension should be carefully selected.

The exclusion criteria was as follows: patients (1) who had other kidney diseases, such as renal cysts, tumors, stones, hydronephrosis and other lesions; (2) whose spectrum of renal interlobar artery could not be accurately detected; and (3) who showed a difference between the highest and lowest ARFI values greater than 3m/sin in the multiple ARFI inspections. After obtaining the intrarenal artery spectrum, the RI and AT values are automatically obtained by the instrument.

In addition, the study recruited 36 healthy volunteers (male: female = 17:19, age range: 16–72 years old) as the normal control group. None of the volunteers in the normal control group were found to have any kidney-related diseases or related clinical symptoms after laboratory and imaging examinations.

This study was approved by the Medical Ethics Committee of the First Affiliated Hospital of Dalian Medical University. Medical ethics committee ethics approval certificate number YJ-KY-FB-2019-75.

Ultrasonic Image Acquisition

First, the Siemens ACUSON S2000 ultrasonography instrument (Siemens Medical Solutions, Mountain View, CA, USA), equipped with a convex array probe of 1–6mhz, was used for ARFI.

Second, the PHILIPS IU Elite ultrasonography diagnostic instrument (PHILIPS Medical Systems, Bothell, USA) was used for 2D and 3D ultrasonography imaging. The C5-1 ventral probe was configured for 2D imaging, and the X6-1 ventral probe was configured for 3D imaging.

Before examination, all patients waited in a quiet room with a temperature of 25 degrees Celsius for 15 minutes. First, ARFI was performed. The patient was asked to lie in the right lateral position, and the kidney was scanned using a convex probe. Patients were asked to hold their breath after calm breathing, and virtual touch quantification was enabled. During ARFI assessment, for standardization, Renal medulla and sinus were carefully excluded from the sample volume. The sample line was perpendicular to the surface of the kidney. Besides, the transducer was located as close to the kidney as possible, with a depth limitation of 8.0 cm. Once the location of transducer and sample volume had been determined, the operator maintained the same position during examination. The applied transducer pressure was minimized as much as possible during imaging to avoid mechanical compression on the kidney. This ARFI protocol was designed to minimize the potential impact of variation of transducer force, sampling error of non-cortical tissue and structural anisotropy of the kidney (¹²Wang et al., 2014).

The region of interest (ROI) was placed in the middle of the kidney and as perpendicular to the renal cortex as possible. The ROI was fixed at 10*6mm² and SWV measurements were expressed in meters per second (¹³Hu et al., 2014). The shear wave velocity of the renal cortex was measured (Fig. 1-b). Five effective measurements were taken for each kidney, and the mean value was obtained. Subsequently, a conventional two-dimensional ultrasound examination was performed using a C5-1 abdominal probe of the PHILIPS IU Elite instrument to record the length of the kidney, the thickness of the cortex, and the internal echo. Effective measurement of interlobular artery spectrum in patients(The angle between the sound beam and the blood flow < 60°),And record the values of RI and AT (Fig. 1-a).

Finally, switch to the X6-1 abdominal probe, scan the patient's longitudinal section of the kidney, obtain a three-dimensional image of the kidney, and collect two effective three-dimensional images from all patients. Subsequently, two experienced ultrasound doctors performed a three-dimensional reconstruction of the patient's kidney image, dividing the long axis of the kidney into 15 sections, drawing

the kidney boundaries of each layer one by one, and then calculating the volume (Fig. 1-c), the final result takes the average of four measurements.

Pathological Assessment

One day later, an ultrasound-guided needle biopsy was performed on the left lower pole of the patient's renal parenchyma. Biopsy specimens were fixed in 4% formaldehyde solution and embedded in paraffin. Then, 2 μ m thick serial sections were cut and applied with hematoxylin-eosin staining method, silver periodate method and Masson-Goldner tricolor method according to standards Dyeing. Each specimen contains at least 10 glomeruli. The pathology assessment was scored by two experienced pathologists who were unaware of the patient's clinical and ultrasound findings. If there is any objection, Follow the principle of negotiation (¹⁴Li et al., 2014; ¹⁵Katafuchi et al., 1998; ¹⁶Hu et al., 2014). The glomerular, tubulointerstitial, and vascular lesions of patients with CKD were scored 12–14 according to the scoring method described by Li et al. According to the pathological score of CKD patients, they were divided into three groups: group 1 was mildly injured group (score \leq 9), group 2 was moderately injured group (9 < score \leq 18), and group 3 was severely injured group. (score > 19) (Table 1).

The pathology was assessed by two experienced pathologists who were unaware of the patients' clinical status and ultrasonography examination. Any discrepancy was resolved by consensus. According to the grading method described by Li et al. the renal glomeruli, renal tubular interstitial and vascular injured in CKD patients were graded. CKD patients were then divided into three groups according to their pathological scores: group 1, the mildly impaired group (score: 9); group 2, the moderately impaired group (score: 9–18); and group 3, the severely impaired group (score: \geq 19).

Statistical processing method

In this study, the categorical variable was expressed as frequency and percentage, and the continuous variable was expressed as mean and standard deviation. The clinical characteristics of the patients and control group were compared using the Mann-Whitney test for the continuous variable and the chi-square test for the categorical variable. A multiple logistic regression model was used to evaluate the correlation between various ultrasonography indicators and renal pathology scores, to calculate the unadjusted odds ratio (OR) and 95 percent confidence interval, and to use a ROC diagnostic curve to diagnose the accuracy of various ultrasonography indicators in diagnosing renal diseases. All analysis used statistical package R (<http://www.R-project.org>, The R Foundation) and statistical software (<http://www.empowerstats.com>, X&Y Solution, Inc Boston, MA).

Results

Basic demographics

The basic characteristics of patients are shown in (Table 2). Of the 118 patients, 31, 39 and 48 presented mild, moderate and severely impaired pathological results, respectively. No significant difference in

gender, age and body mass index (BMI) was discovered between the different groups ($P > 0.05$). In patients with mild impairment, creatinine did not show a significant difference from that of normal patients ($P > 0.05$), but in patients with moderate or severe impairment, the creatinine level was significantly higher than normal patients ($P < 0.01$). In conclusion, the patient's e-GFR showed a significant decrease with the increase of pathological injure ($P < 0.05$).

2D and 3D ultrasound imaging and ARFI.

The basic results of the ultrasonography and the multiple logistic regression analysis of corresponding pathological results of CKD patients are shown in (Figures 1-b and 1-c), respectively. As seen in (Table 2), only the interlobar artery AT showed a statistical difference ($P < 0.05$) when compared with the control group. Although the shear wave elastography decreased in value, it was not statistically significant. All ultrasonography indicators, such as shear wave elasticity imaging (SWV), renal length, renal parenchymal thickness, 3D renal volume and renal interlobar artery RI and AT, showed significant differences in moderate and severe renal pathological damage ($P > 0.05$).

As seen in (Table 3)^(17Boddi,M.,1996), the multiple logistic regression analysis showed a significant correlation between the pathological results and renal interlobar artery AT (group 1, OR: 21.43 [4.64, 38.22]; group 2, OR: 33.77 [14.11, 53.43]; group 3, OR: 26.28 [9.98, 42.57]). After adjusting for confounding variables, the predictive efficacy of AT increased (group 1, OR: 35.69 [18.55, 52.83]; group 2, OR: 36.61 [16.00, 57.21]; group 3, OR: 34.45 [12.40, 56.49]), which means that only renal interlobar artery AT was an effective predictor in the mildly impaired group. In patients with moderate injured, despite significant differences in SWV, renal length, renal parenchymal thickness, renal 3D volume and renal interlobar artery RI, multiple logistic regression analysis indicated that only AT (OR: 33.77 [14.11, 53.43]) and RI (OR: 19.59 [9.36, 29.83]) were effective predictors. Kidney length (OR: -1.62 [-2.06, -1.19]), 3D renal volume (OR: -0.05 [-0.07, -0.03]) and renal interlobar artery RI (OR: 16.75 [2.80, 30.70]) and AT (OR: 26.28 [9.98, 42.57]) were all effective predictors in severely injured CKD patients. Although the renal SWV showed significant statistical difference between moderate and severe injured, the OR value of the severely injured group was - 1.70 (-3.13, -0.28) before and after the adjustment of confounding variables. was not statistically significant.

Diagnostic performance of ultrasonography indexes in early CKD injure

As shown in (Table 4), the diagnostic efficacy of AT (AUC: 84.2 [74,693.7]) was superior to other ultrasonography indicators in CKD patients with mild pathological injured. The optimal cut-off point for mild renal injure diagnosed AT CKD was 0.083s (Figs. 2). In addition, the sensitivity of SWV to detect mild renal injure (83.8 percent) was highest among all ultrasonography indicators.

Discussion And Conclusions

In the current study, the level of renal interlobar artery AT was significantly correlated with the degree of the pathological injure of CKD. Acceleration time (AT) is one of the presence of injure Doppler waveform

and a slow rise to peak systole in spectral Doppler of the interlobar artery, and it is commonly used as an indirect indicator for the diagnosis of renal artery stenosis, acute renal failure, and transplant rejection^(18Li et al., 2008; 19-20Wong et al., 1989; 21Bardelli et al., 2006; 22Ripolles et al., 2001). This phenomenon is called "Tardus-parvus" effect^(23Zhu et al., 2018). Tardus means slow and late and Parvus means small and little. Tardus refers to the fact that systolic acceleration of the waveform is slow with consequent increase in time to reach the systolic peak. Parvus refers to the fact that the systolic peak is of low height indicating a slow velocity^(24Bude et al., 1994). At present, no study exists to prove the relationship between the prolongation of renal interlobar artery AT and chronic renal injury. Chronic nephropathy is pathologically a relatively uniform reaction, and the progressive decline of renal function is characterized by the destruction of microvascular structure and the accumulation of fibrotic matrix^(25Lopez-Novoa et al., 2011). The destruction of microvascular structure (microvascular wall thickening, arterial wall transparency change, etc.) leads to the loss of effective micro-vessels and injury of microcirculation, which affects the hemodynamic changes of renal interlobar arteries^(26Ali et al., 2016). In spectral doppler the AT of renal interlobar arteries is extended. In addition, as the degree of renal injury increases, the injury of microcirculation increases continuously, and the AT of renal interlobar arteries also increases significantly. Therefore, in this study, the AT of renal interlobar arteries was an effective predictor of the degree of renal injury.

At present, resistance index (RI) is a doppler parameter that provides information about vascular activity and total vascular impedance of parenchymal circulation. Although the RI is affected by multiple factors, such as in diseases causing the pressure differential between systole and diastole^(12Tublin et al., 1999), RI is one of the Doppler parameters that provides information about arterial impedance, theoretically, the RI expresses vascular resistance, it can reflect flow^(27Sigirci et al., 2006). It has been shown that renal vascular RI changes with age. According to Meola M. et al^(3Meola, M;2008), if the microcirculation was not significantly injured, the renal vascular resistance in the initial stage of ischemia was very low ($RI < 0.60$). These findings were consistent with the results of this study. In kidneys with mild injury, the microcirculation was slightly injured, and RI showed no significant difference. However, RI showed statistical significance in cases of moderate and severe injury.

As CKD progresses, the degree of fibrosis increases. Shear wave elastography was the ARFI technology used as an indicator to detect tissue hardness. In this study, although the SWV value ($2.54 + 0.65$) of early injury was slightly lower than that of the normal control group ($2.70 + 1.04$), the difference was not statistically significant. Therefore, SWV was not an independent predictor of chronic renal injury, which was consistent with previous studies by Wang et al^(12Wang et al., 2014). However, in the study by Hu et al. Combined with the observed pathological results, it was found in this study that patients with early renal injury presented pathological changes such as glomerulosclerosis and Capillary sclerosis, and the elasticity of the kidney detected by elastography was higher than that of the normal control group, so the SWV value of elasticity was reduced, which was consistent with the prediction in the study of Hu et al^(28Gilja et al., 1995). SWV not only assessed renal fibrosis, but levels of SWV also significantly differed among different degrees of injury ($P < 0.05$). In addition, some studies^{(29Guo et al., 2013; 30Bob et al.,}

2015) assessed the relationship between SWV levels and e-GFR and concluded that ARFI might be a potentially useful tool for detecting different stages of renal disease. The negative results of the current study might be related to pathological changes prior to test indicators (such as creatinine, e-GFR, etc.), structural heterogeneity of renal parenchyma, individual differences of operators and operational repeatability of SWV (³¹Bob et al., 2014). In this study, it was considered that ultrasonography elastography could not be used as an independent predictor of early chronic kidney disease, resulting in negative results of this conclusion.

Just as traditional 2D ultrasonography imaging can provide accurate information such as renal size and thickness of renal parenchyma, 3D renal imaging also improves the accuracy of renal volume detection (²⁸Gilja et al., 1995). which is of obvious significance in the case of severe irreversible injure to the kidney. In this study, renal length (OR: -1.62 [-2.06, -1.19]) and renal 3D volume (OR: -0.05 [-0.07, -0.03]) showed significant differences in severe renal injure, even after adjusting for confounding variables such as gender, age and BMI. This result indicated that renal volume and renal length were effective parameters for the assessment of severe renal injure and showed a negative correlation, which was consistent with the study by Xu et al in 2018 (³²Xu et al., 2018). However, in early and moderate pathological injure, the results showed that the pathological structural injure had not caused significant morphological changes, and the individual differences between kidneys were relatively large. Therefore, the renal volume and length did not show statistical significance.

The limitations of this study were as follows: (1) Patients admitted to the First Affiliated Hospital of Dalian Medical University were selected for this study, which may have indicated certain selection bias due to the regional and economic characteristics of the disease. (2) This study was a single-center small sample study. However, the kidney is different from the thyroid or liver, and its individual differences are relatively large. Although this study considered that renal interlobar artery AT was an effective factor to predict renal injure, these results need to be verified by a large multi-center sample. Due to the small sample size, this study was not classified according to different pathological types, and whether differences in CKD of different pathological types exist during ultrasonography examination remains unsolved. (3) Plus, due to the limitations of medical ethics, Kidney biopsy cannot be performed at multiple centers in large samples.

Conclusions

The AT of the renal interlobar artery was significantly correlated with the degree of pathological injure of CKD. To detect severe renal injure, 3D ultrasonography imaging can be used. ARFI was not significantly correlated with chronic renal injure, but ARFI had the highest sensitivity (83.8 percent) when diagnosing minor renal injure. Therefore, the AT of the renal interlobar artery can be used to predict mild injure from CKD, which has higher diagnostic performance than other 2D, 3D ultrasonography imaging or ARFI. In addition, ARFI can be used to increase AT sensitivity to diagnose slightly injured kidneys.

Abbreviations

two-dimensional (2D)

three-dimensional (3D)

shear wave elasticity imaging [SWV]

acoustic radiation force pulse imaging (ARFI)

Renal interlobar artery acceleration time (AT)

Chronic kidney disease (CKD)

area under curve [AUC]

the Kidney Disease Prognosis Quality Initiative (K/DPQI)

estimated glomerular filtration rate (e-GFR)

region of interest (ROI)

odds ratio (OR)

resistance index (RI)

Declarations

-Ethical Approval

This study was approved by the Medical Ethics Committee of the First Affiliated Hospital of Dalian Medical University.

-Consent to Participate

The author acknowledges: "All authors read and approved the final manuscript and agreed to publish it".

-Consent to Publish All author's interests are not conflict and agree to submit their papers for publication.

-Funding instructions: Project number 20170540256 Natural science foundation of Liaoning.

-Availability of data and materials.

All data generated or analyzed in this study are included in this article.

The data set generated and/or analyzed in the current study cannot be made public but can be obtained from the corresponding author under reasonable request.

Authors' Contributions:

Yanli Huang, MM: Design/Drafting article

Xiaohang Wu, MM: Concept

Ye Tao, MM: Data analysis/interpretation

Jialing Wu, MM: Interpretation of data

Yumei Yan, MD: Critical revision of article

Mengyan Ma, MM: Retrieval and analysis of literature

Xinyue Yuan, MM: Statistics

Fengfei Li, MM :Data collection

Xiukun Hou, Prof*: Approval of the submitted and final versions.

All authors have read and approved the manuscript.

Acknowledgements

Thanks to the case file management teacher for this study.

References

1. Bello AK, Levin A and Tonelli M, et al. Assessment of Global Kidney Health Care Status. *JAMA* 2017; 317: 1864–1881. Journal Article. DOI: 10.1001/jama.2017.4046.
2. Meola M and Petrucci I. Color Doppler sonography in the study of chronic ischemic nephropathy. *J Ultrasound* 2008; 11: 55–73. Journal Article. DOI: 10.1016/j.jus.2008.03.006.
3. Meola M and Petrucci I. Color Doppler sonography in the study of chronic ischemic nephropathy. *J Ultrasound* 2008; 11: 55–73. Journal Article. DOI: 10.1016/j.jus.2008.03.006.
4. Muntner P, Judd SE and McClellan W, et al. Incidence of stroke symptoms among adults with chronic kidney disease: results from the REasons for Geographic And Racial Differences in Stroke (REGARDS) study. *Nephrol Dial Transplant* 2012; 27: 166–173. Journal Article; Research Support, N.I.H., Extramural; Research Support, Non-U.S. Gov't. DOI: 10.1093/ndt/gfr218.
5. Mandayam S and Winkelmayr WC. Worldwide Preparedness for Kidney Health Care. *JAMA* 2017; 317: 1838–1839. Editorial; Comment. DOI: 10.1001/jama.2017.2825.
6. Boor P, Sebekova K and Ostendorf T, et al. Treatment targets in renal fibrosis. *Nephrol Dial Transplant* 2007; 22: 3391–3407. Editorial; Research Support, Non-U.S. Gov't; Review. DOI: 10.1093/ndt/gfm393.
7. de Amorim PC, de Mello JC and Guimaraes FH, et al. Reproducibility of renal volume measurement in adults using 3-dimensional sonography. *J Ultrasound Med* 2014; 33: 431–435. Journal Article;

- Observational Study. DOI: 10.7863/ultra.33.3.431.
8. Nightingale K. Acoustic Radiation Force Impulse (ARFI) Imaging: a Review. *Curr Med Imaging Rev* 2011; 7: 328–339. Journal Article. DOI: 10.2174/157340511798038657.
 9. Nightingale K, Soo MS and Nightingale R, et al. Acoustic radiation force impulse imaging: in vivo demonstration of clinical feasibility. *Ultrasound Med. Biol.* 2002; 28: 227–235. Journal Article; Research Support, U.S. Gov't, Non-P.H.S.; Research Support, U.S. Gov't, P.H.S. DOI: 10.1016/s0301-5629(01)00499-9.
 10. Su TH, Liao CH and Liu CH, et al. Acoustic Radiation Force Impulse US Imaging: Liver Stiffness in Patients with Chronic Hepatitis B with and without Antiviral Therapy. *Radiology* 2018; 288: 293–299. Journal Article; Research Support, Non-U.S. Gov't. DOI: 10.1148/radiol.2018171116.
 11. Brancaforte A, Serantoni S and Silva BF, et al. Renal volume assessment with 3D ultrasound. *Radiol Med* 2011; 116: 1095–1104. Comparative Study; Journal Article. DOI: 10.1007/s11547-011-0691-8.
 12. Tublin ME, Tessler FN and Murphy ME. Correlation between renal vascular resistance, pulse pressure, and the resistive index in isolated perfused rabbit kidneys. *Radiology* 1999; 213: 258–264. Journal Article; Research Support, Non-U.S. Gov't. DOI: 10.1148/radiology.213.1.r99oc19258.
 13. Hu Q, Wang XY and He HG, et al. Acoustic radiation force impulse imaging for non-invasive assessment of renal histopathology in chronic kidney disease. *Plos One* 2014; 9: e115051. Comparative Study; Evaluation Studies; Journal Article; Research Support, Non-U.S. Gov't. DOI: 10.1371/journal.pone.0115051.
 14. Li Q, Li J and Zhang L, et al. Diffusion-weighted imaging in assessing renal pathology of chronic kidney disease: A preliminary clinical study. *Eur. J. Radiol.* 2014; 83: 756–762. Journal Article. DOI: 10.1016/j.ejrad.2014.01.024.
 15. Katafuchi R, Kiyoshi Y and Oh Y, et al. Glomerular score as a prognosticator in IgA nephropathy: its usefulness and limitation. *Clin. Nephrol.* 1998; 49: 1–8. Journal Article.
 16. Chen LH, Advani SL and Thai K, et al. SDF-1/CXCR4 signaling preserves microvascular integrity and renal function in chronic kidney disease. *Plos One* 2014; 9: e92227. Journal Article; Research Support, Non-U.S. Gov't. DOI: 10.1371/journal.pone.0092227.
 17. Boddi M, Sacchi S and Lammel RM, et al. Age-related and vasomotor stimuli-induced changes in renal vascular resistance detected by Doppler ultrasound. *Am. J. Hypertens.* 1996; 9: 461–466. Clinical Trial; Journal Article. DOI: 10.1016/0895-7061(96)00027-1.
 18. Li JC, Jiang YX and Zhang SY, et al. Evaluation of renal artery stenosis with hemodynamic parameters of Doppler sonography. *J. Vasc. Surg.* 2008; 48: 323–328. Journal Article; Research Support, Non-U.S. Gov't. DOI: 10.1016/j.jvs.2008.03.048.
 19. Wang L, Xia P and Lv K, et al. Assessment of renal tissue elasticity by acoustic radiation force impulse quantification with histopathological correlation: preliminary experience in chronic kidney disease. *Eur. Radiol.* 2014; 24: 1694–1699. Journal Article; Research Support, Non-U.S. Gov't. DOI: 10.1007/s00330-014-3162-5.

20. Wong SN, Lo RN and Yu EC. Renal blood flow pattern by noninvasive Doppler ultrasound in normal children and acute renal failure patients. *J Ultrasound Med* 1989; 8: 135–141. Comparative Study; Journal Article. DOI: 10.7863/jum.1989.8.3.135.
21. Bardelli M, Veglio F and Arosio E, et al. New intrarenal echo-Doppler velocimetric indices for the diagnosis of renal artery stenosis. *Kidney Int.* 2006; 69: 580–587. Comparative Study; Journal Article; Multicenter Study. DOI: 10.1038/sj.ki.5000112.
22. Ripolles T, Aliaga R and Morote V, et al. Utility of intrarenal Doppler ultrasound in the diagnosis of renal artery stenosis. *Eur. J. Radiol.* 2001; 40: 54–63. Comparative Study; Evaluation Studies; Journal Article. DOI: 10.1016/s0720-048x(00)00263-1.
23. Zhu R, Xu Z and Qi Z, et al. How to diagnose renal artery stenosis correctly using ultrasound? Evaluation of results of renal arteries duplex ultrasonography examinations. *Med Ultrason* 2018; 20: 298–305. Journal Article. DOI: 10.11152/mu-1341.
24. Bude RO, Rubin JM and Platt JF, et al. Pulsus tardus: its cause and potential limitations in detection of arterial stenosis. *Radiology* 1994; 190: 779–784. Journal Article. DOI: 10.1148/radiology.190.3.8115627.
25. Lopez-Novoa JM, Rodriguez-Pena AB and Ortiz A, et al. Etiopathology of chronic tubular, glomerular and renovascular nephropathies: clinical implications. *J. Transl Med* 2011; 9: 13. Journal Article; Review. DOI: 10.1186/1479-5876-9-13.
26. Ali ZA, Karimi GK and Nazif T, et al. Imaging- and physiology-guided percutaneous coronary intervention without contrast administration in advanced renal failure: a feasibility, safety, and outcome study. *Eur. Heart J.* 2016; 37: 3090–3095. Journal Article. DOI: 10.1093/eurheartj/ehw078.
27. Sigirci A, Hallac T and Akyncy A, et al. Renal interlobar artery parameters with duplex Doppler sonography and correlations with age, plasma renin, and aldosterone levels in healthy children. *AJR Am J Roentgenol* 2006; 186: 828–832. Comparative Study; Journal Article. DOI: 10.2214/AJR.04.1445.
28. Gilja OH, Smievoll AI and Thune N, et al. In vivo comparison of 3D ultrasonography and magnetic resonance imaging in volume estimation of human kidneys. *Ultrasound Med. Biol.* 1995; 21: 25–32. Comparative Study; Journal Article; Research Support, Non-U.S. Gov't. DOI: 10.1016/0301-5629(94)00082-4.
29. Guo LH, Xu HX and Fu HJ, et al. Acoustic radiation force impulse imaging for noninvasive evaluation of renal parenchyma elasticity: preliminary findings. *Plos One* 2013; 8: e68925. Journal Article; Research Support, Non-U.S. Gov't. DOI: 10.1371/journal.pone.0068925.
30. Bob F, Bota S and Sporea I, et al. Relationship between the estimated glomerular filtration rate and kidney shear wave speed values assessed by acoustic radiation force impulse elastography: a pilot study. *J Ultrasound Med* 2015; 34: 649–654. Journal Article. DOI: 10.7863/ultra.34.4.649.
31. Bob F, Bota S and Sporea I, et al. Kidney shear wave speed values in subjects with and without renal pathology and inter-operator reproducibility of acoustic radiation force impulse elastography (ARFI)–preliminary results. *Plos One* 2014; 9: e113761. Journal Article. DOI: 10.1371/journal.pone.0113761.

32. Xu J, Hwang SI and Lee HJ, et al. Relationship of renal morphology on 3-dimensional ultrasonography with renal pathologic findings and outcome in biopsy-proven nephropathy. *Exp Ther Med* 2018; 15: 2088–2096. Journal Article. DOI: 10.3892/etm.2017.5626.

Tables

Table 1. Criteria for renal pathology score

score	Glomerular score (3-12 points)			Tubulointerstitial score (3-9 points)			Vascular score (2-6 points)	
	Glomerular hypercellularity	Glomerular segmental lesions	Glomerular sclerosis	Interstitial cell infiltration	Interstitial fibrosis	Tubular atrophy	Vessel wall thickening	Arterial hyaline change
1	<25%	<10%	<10%	<25%	<25%	<25%	<10%	<10%
2	25%-50%	10%-25%	10%-25%	25%-50%	25%-50%	25%-50%	10%-25%	10%-25%
3	>50%-75%	>25%-50%	>25%-50%	>50%	>50%	>50%	>25%	>25%
4	>75%	>50%	>50%	NA	NA	NA	NA	NA

NA= not applicable

Arterial hyaline change is a transparent denaturation, also known as hyaline change. The blood vessel intima becomes more transparent after being damaged, and the plasma protein infiltrates under the intima and coagulates under the endothelial cells, which is a damaging change.

Table 2. basic characteristics of the study population

Variable	Controls	Cases		
	0 (n=36)	1 (n=31)	2 (n=39)	3 (n=48)
Male sex, No.(%)	17(47.2)	15(48.4)	26(66.7)	26(54.2)
Age, yr	46.2±17.0	45.3±15.1	54.8±13.3	54.5±13.8
BMI, kg/m ²	22.9±3.4	22.7±3.8	23.8±3.7	22.7±3.5
e-GFR, ml/min.1.73m ²	134.51±29.96	111.02±22.60 ^a	56.94±22.78 ^{a, f}	20.75±18.40 ^{c, f, i}
Serum creatinine, umol/L	55.03±10.00	66.48±20.02	127.74±89.57 ^{b, f}	449.35±342.32 ^{c, f, i}
Hypertensive, No. (%)	4(11.1)	15(48.4)	22(56.4)	31(64.6)
Diabetics, No. (%)	2(5.6)	11(35.5)	20(51.2)	26(54.1)
SWV, m/s	2.70±1.04	2.54±0.65	2.24±0.67 ^{a, d}	1.93±0.63 ^{b, e, g}
SWV-depth, cm	4.24±1.19	4.44±1.13	4.75±1.13	5.13±1.28
Renal length, mm	109.98±9.47	113.55±10.84	105.49±10.38 ^e	89.99±14.71 ^{c, f, i}
Parenchymal thickness, mm	16.09±2.29	16.25±2.75	14.42±2.01 ^e	13.15±2.40 ^{h, f}
Renal volume, mm ³	181.39±56.72	178.80±57.83	150.90±35.84 ^d	109.34±39.46 ^{c, f, i}
Interlobar arterial RI	0.56±0.09	0.54±0.08	0.60±0.07 ^{b, e}	0.66±0.06 ^{a, f, g}
Interlobar arterial AT, s	0.067±0.023	0.107±0.033 ^a	0.144±0.035 ^{b, f}	0.154±0.052 ^{b, f}

Plus-minus values are means ±SD.

P values were calculated by comparing characteristics between with controls: ^aP<0.05, ^bP<0.01, ^cP<0.001; comparing with group 1: ^d P<0.05, ^eP<0.01, ^fP<0.001; comparing with group 2:^g P<0.05, ^hP<0.01, ⁱP<0.001

BMI denotes body mass index

RI denotes resistance index

AT denotes acceleration time

Patients with hypertension are defined as patients with a previous systolic blood pressure of ≥ 140 mmHg and / or a diastolic blood pressure of ≥ 90 mmHg.

Diabetes is defined as meeting the criteria proposed by the International General WHO Expert Committee on Diabetes.

Table 3. Multivariate regression analysis to evaluate the ultrasonic characteristics of the normal group and the control group

Variable	Controls		Cases		
	0	1	2	3	
	(n=36)	(n=31)	(n=39)	(n=48)	
SWV, m/s	Crude	Ref	-0.27 (-1.21, 0.67)	-0.69 (-1.86, 0.47)	-1.70 (-3.13, -0.28)
	Adjusted ^b	Ref	0.39 (-0.63, 1.42)	-0.36 (-1.98, 1.26)	-1.30 (-2.98, 0.38)
Renal length, mm	Crude	Ref	-0.15 (-0.71, 0.42)	-0.49 (-1.24, 0.26)	-1.62(-2.06, -1.19)
	Adjusted ^a	Ref	-0.06 (-0.64, 0.51)	-0.73 (-1.52, 0.06)	-1.70(-2.12, -1.27)
Parenchymal thickness, mm	Crude	Ref	-0.10 (-0.32, 0.13)	-0.19 (-0.58, 0.21)	-0.22 (-0.61, 0.17)
	Adjusted ^a	Ref	-0.09 (-0.32, 0.14)	-0.20 (-0.60, 0.21)	-0.25 (-0.64, 0.14)
Renal volume, mm ³	Crude	Ref	0.00 (-0.01, 0.01)	-0.01 (-0.03, 0.02)	-0.05(-0.07, -0.03)
	Adjusted ^a	Ref	0.00 (-0.01, 0.01)	-0.01 (-0.03, 0.01)	-0.05(-0.07, -0.03)
Interlobar arterial RI	Crude	Ref	3.30 (-4.04, 10.63)	19.59 (9.36, 29.83)	16.75 (2.80, 30.70)
	Adjusted ^a	Ref	5.88 (-1.55, 13.30)	19.33 (7.96, 30.70)	20.42 (5.78, 35.05)
Interlobar arterial AT, s	Crude	Ref	21.43 (4.64, 38.22)	33.77 (14.11, 53.43)	26.28 (9.98, 42.57)
	Adjusted ^a	Ref	35.69 (18.55, 52.83)	36.61 (16.00, 57.21)	34.45 (12.40, 56.49)

^aAdjusted for Age, Sex, BMI.

^bAdjusted for Age, Sex, BMI, SWV-depth.

Table 4. ROC analysis of renal disease detected by ultrasound in group 1 (mildly impaired group)

	AUC, percent(95% CI)	cut-off point	Sensitivity, percent	Specificity, percent	Accuracy, percent
SWV, m/s	55.5 (41.3 69.8)	3.13	83.8	41.7	61.2
Renal length, mm	60.3 (46.2 74.3)	11.25	54.8	72.2	64.2
Parenchymal thickness, mm	52.7 (38.4 67.0)	16.3	52.8	61.3	56.7
Renal volume, mm ³	50.0 (35.8 64.3)	112.5	19.3	91.7	58.2
Interlobar arterial RI	58.0 (44.1 71.8)	0.61	80.7	41.7	59.7
Interlobar arterial AT, s	84.2 (74,6 93.7)	0.083	77.4	80.6	79.1

Figures

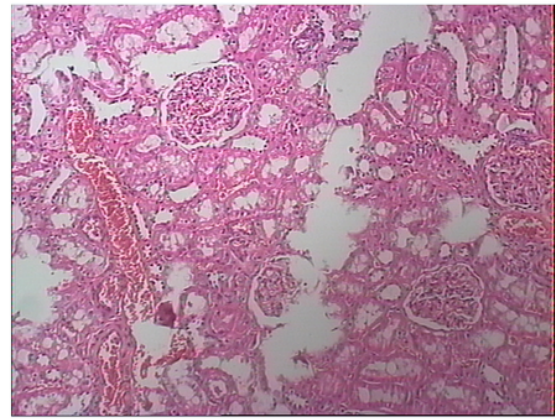
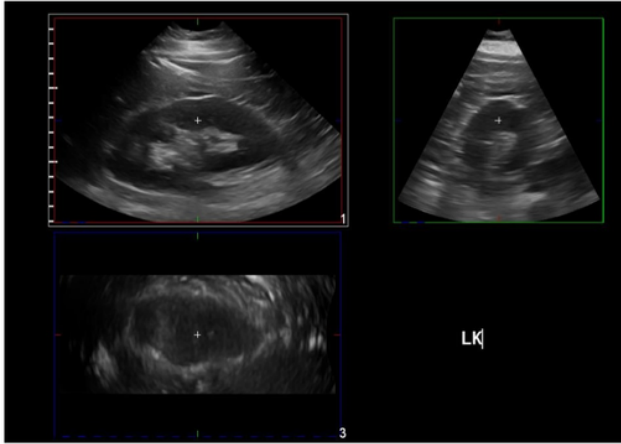
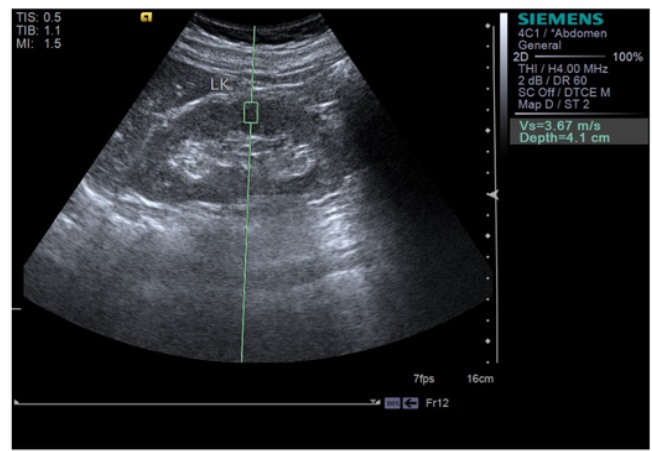
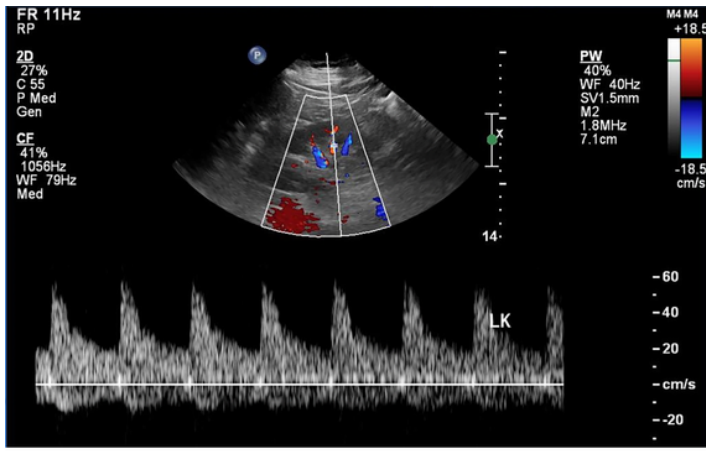


Figure 1

a. Interlobular artery spectrum b. ARFI images, and the SWV values were 3.67 m/s c. Renal volume images d. Neuropathologic Image for histopathology. Microscopy revealed mild glomerular lesions, diffuse proliferation of mesangial cells and stromal matrix, basement membrane vacuolar degeneration, mesangial eosinophilic protein deposition, tubular vacuolar granulation degeneration, renal interstitial focal lymphoid mononuclear cell infiltration, and minor glomerular lesions.

ROC curve In Group 1

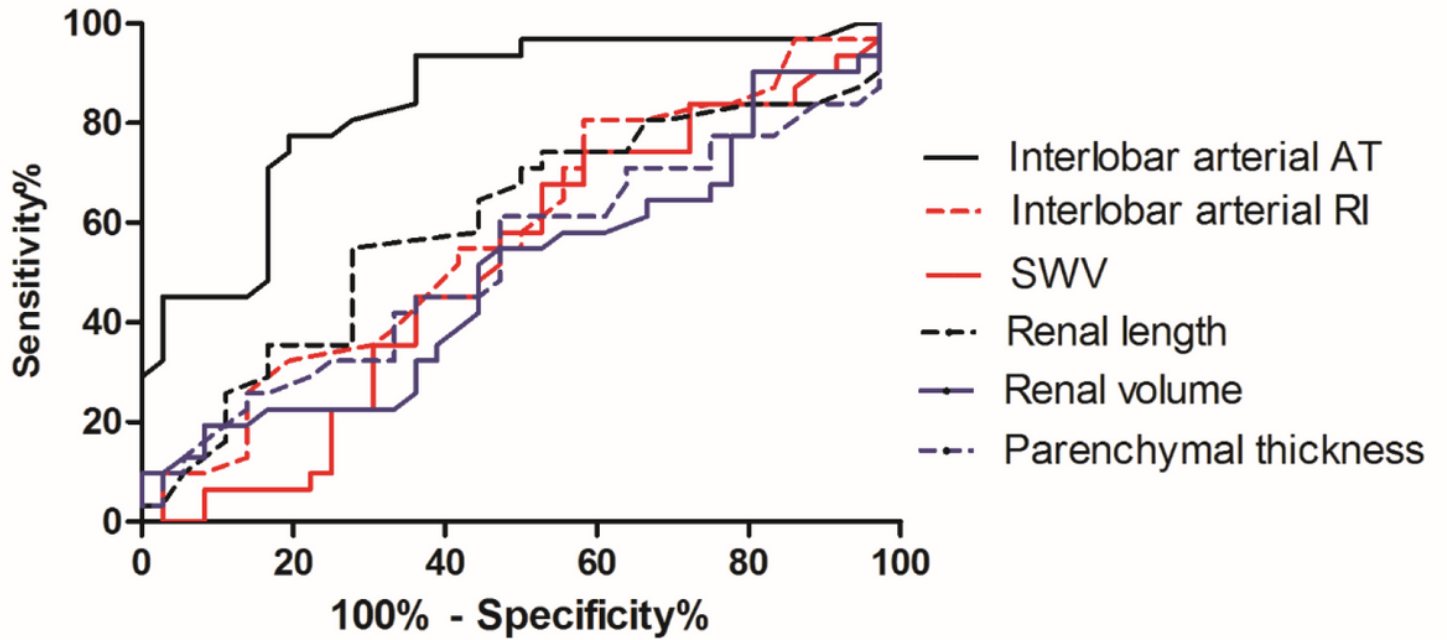


Figure 2

Predictive performance of the receiver operating characteristic (ROC) curves of those ultrasound parameters in table 4.